HAL open science

A detailed high-pressure oxidation study of di-isopropyl ether

Zeynep Serinyel, Maxence Lailliau, Guillaume Dayma, Philippe Dagaut

To cite this version:

Zeynep Serinyel, Maxence Lailliau, Guillaume Dayma, Philippe Dagaut. A detailed high-pressure oxidation study of di-isopropyl ether. Proceedings of the Combustion Institute, 2023, 39 (1), pp.561-569. 10.1016/j.proci.2022.07.038 . hal-04121031

HAL Id: hal-04121031

https://cnrs.hal.science/hal-04121031v1

Submitted on 7 Jun 2023

HAL is a multi-disciplinary open access archive for the deposit and dissemination of scientific research documents, whether they are published or not. The documents may come from teaching and research institutions in France or abroad, or from public or private research centers.

L'archive ouverte pluridisciplinaire **HAL**, est destinée au dépôt et à la diffusion de documents scientifiques de niveau recherche, publiés ou non, émanant des établissements d'enseignement et de recherche français ou étrangers, des laboratoires publics ou privés.

Copyright

A detailed high-pressure oxidation study of di-iso-propyl ether

Zeynep Serinyel[a,b*], Maxence Lailliau[b], Guillaume Dayma[a,b], Philippe Dagaut[b]

[a] *UFR Sciences et Techniques, Université d'Orléans, rue de Chartres, 45100 Orléans*
[b] *CNRS–ICARE, 1C avenue de la Recherche Scientifique, 45071 Orléans cedex 2*

Abstract

The oxidation of di-iso-propyl-ether (DIPE) was studied in a jet-stirred reactor. Fuel-lean, stoichiometric, and fuel-rich mixtures (φ = 0.5–4) were oxidized at a constant fuel mole fraction of 1000 ppm, at temperatures ranging from 500 to 1160 K, at 10 atm, and constant residence time of 0.7 s. The chosen conditions are consistent with our previous studies on ether oxidation. Mole fraction profiles were obtained through sonic probe sampling, and analyzed by gas chromatography and Fourier transform infrared spectrometry. As opposed to our previous studies on ethers (S. Thion et al. 2017, Z. Serinyel et al. 2018 and 2020), DIPE showed no low-temperature reactivity. Oxidation of the rich mixture showed similarities to pyrolysis producing important quantities of propene and iso-propanol, while no iso-propanol is observed under lean conditions. In terms of overall reactivity, DIPE showed smaller fuel conversion compared to other symmetric ethers previously studied. The present data and literature experiments were simulated with our ether oxidation mechanism showing good agreement.

Keywords: isopropyl ether; jet-stirred reactor; oxidation; chemical kinetics

*Corresponding author.

1. Introduction

In an effort to understand the oxidation and pyrolysis behavior of ethers, systematic experimental and modeling studies have been being conducted within our team [1-6]. Oxidation of di-iso-propyl ether (DIPE) has been studied in this context, in the same experimental conditions as diethyl, di-n-propyl and di-n-butyl ethers, in order to make a comparison possible. These previous studies consisted in symmetric unbranched ethers, which all showed an important reactivity at low temperatures (between 450 and 750 K).

DIPE has an interesting character as it is considered as an octane improver, due its branched nature [7], high octane number and low solubility in water [8]. Its oxidation was previously studied in a jet-stirred reactor by Goldaniga et al. [9] in 1998, along with other octane improvers such as methyl and ethyl tertiary butyl ethers (MTBE, ETBE) and tertiary amyl-methyl ether (TAME), at high pressure. In that study, while TAME oxidation was reported in detail, only formaldehyde and iso-butene mole fraction profiles were provided for DIPE oxidation. More recently, Fan et al. [10] studied DIPE oxidation in a jet-stirred reactor at atmospheric pressure and for a stoichiometric mixture at a constant residence time of 2 s. Also Hashimoto et al. reported flame extinction limits of DIPE as well as those of ETBE and TAME in a counterflow burner [11]. In terms of engine studies, DIPE was found to decrease the knocking tendency in an HCCI engine and to expand the operating range of HCCI combustion [12].

The present study will complement our systematic investigation, bringing new detailed data at high pressure for this branched symmetric ether.

2. Experimental set-up and kinetic modeling

2.1 Experimental

Experiments were carried out in a fused silica jet-stirred reactor settled inside a stainless-steel pressure resistant jacket. An electrical oven enabled to perform experiments up to 1280 K. The temperature within the reactor was continuously monitored by a Pt/Pt-Rh 10% (S-type) thermocouple located inside a thin wall fused silica tube to prevent catalytic reactions on the metallic wires. Initial fuel mole fraction was 0.1 % for all experiments. Experimental pressure was 10 atm and the residence time (τ) was 0.7 s. The residence time was held constant by adjusting the flow rates at each temperature. The reactive mixtures were highly diluted by nitrogen to avoid high heat release inside the reactor. The liquid fuel was atomized by a nitrogen flow and vaporized through a heated chamber. Reactants were brought separately to the reactor to avoid premature reactions and then injected by 4 injectors providing stirring. Flow rates of the diluent and reactants were controlled by mass flowmeters. A low-pressure sonic probe was used to freeze the reactions and take samples of the reacting mixtures.

Online analyses were performed after sending the samples via a heated line to a Fourier transform infrared (FTIR) spectrometer for the quantification of H_2O, CO, CO_2, and CH_2O. Samples were also stored at ca. 40 mbar in Pyrex bulbs for further analyses using gas chromatography (GC). Two gas chromatographs with a flame ionization detector (FID) were used: one equipped with a DB624 column to quantify oxygenated compounds and the other one with a CP-Al_2O_3/KCl column to quantify hydrocarbons. Identification of the products was done by GC/MS on a Shimadzu GC2010 Plus, with electron impact (70 eV) as the ionization mode. Mole fraction profiles of H_2 were measured using a GC-TCD (thermal conductivity detector) equipped with a CP-CarboPLOT P7 column. The species quantified in this study include di-iso-propyl-ether (DIPE), H_2, H_2O, CO, CO_2, ethylene, methane, ethane, propene, formaldehyde, acetaldehyde, acetone and traces of 1-butene and acetylene. The carbon balance was checked for each sample and the deviation was found to be typically within ±10–15%.

2.2 Kinetic mechanism

We have recently included pyrolysis reactions in our kinetic reaction mechanism [1], and the same mechanism was used in the present work. In the conditions of this study, and in contrast to the pyrolysis experiment [1], hydrogen abstraction reactions from the fuel by OH and HO_2 radicals will be important.

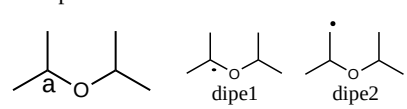

Figure 1. Structure of di-iso-propyl ether

The structure of DIPE and its radicals are illustrated in Fig 1. H-abstraction reaction rate constants by OH radicals were estimated by analogy to the calculations of Zhou et al. [13] on iso-propyl methyl ether for the α–site. For the β–site, which involves 12 equivalent C–H bonds, the estimation (fit) was based on the calculations reported by Zador [14], Zhou [15], Truhlar [16] and co-workers' calculations on the δ–site of 1-butanol as well as Droege and Tully's work on n-butane [17]. This fit is then slowed down by a factor of 2 in order to take into account the fact that the beta C–H bond is slightly stronger (around 102 kcal.mol^{-1}) than that in the δ–position in 1-butanol, which itself is equivalent to a primary C–H bond in an alkane.

H-abstraction reaction rate constants by HO_2 radicals were estimated by analogy with the calculations of Mendes and co-workers [18] on isopropyl methyl ether, with no modification as the C–H sites are comparable.

The JSR simulations were carried out with the Perfectly Stirred Reactor (PSR) code of Chemkin II package [19]. Results are shown in the following section.

3. Results and discussion

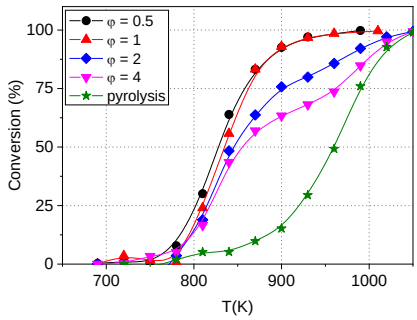

Figure 2. Fuel conversion of DIPE at all equivalence ratios. Pyrolysis data is from [1].

3.1 *Results and model comparison*

Experimental fuel conversion for all experiments as well as the pyrolysis profile from [1] are presented in Figure 2.

Clearly no reactivity is observed at low temperature (T < 750 K). Experiments were extended to 500 K for the lean mixture, where no fuel conversion occurred. The reactivity of DIPE begins at temperatures higher than 770 K and full conversion is observed around 1050 K under present operating conditions. One can also observe a change of slope for the φ = 4 mixture (and to a lesser extent for φ = 2) while the lean and stoichiometric mixtures behave similarly with a slightly higher fuel conversion for the lean case. Obviously, under pyrolysis conditions, fuel conversion is much less at a given temperature: For example at 900 K, only 15% of the fuel is converted under pyrolytic conditions while this is > 60% in oxidation. Nevertheless, DIPE is fully converted regardless of the O_2 content when the temperature reaches 1050 K.

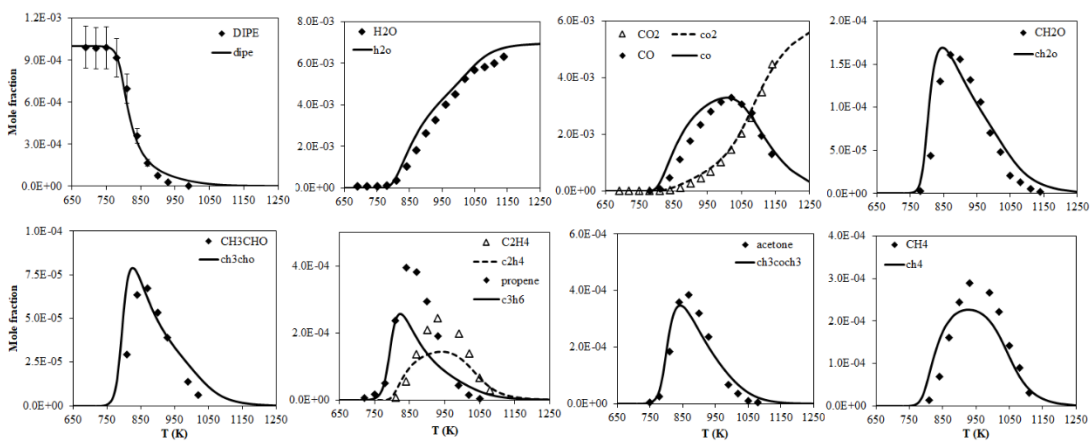

Figure 3. Mole fraction profiles for the φ = 0.5 mixture, P = 10 atm, $X_{0,fuel}$ = 0.1%, τ = 0.7 s (symbols: data, lines: simulations)

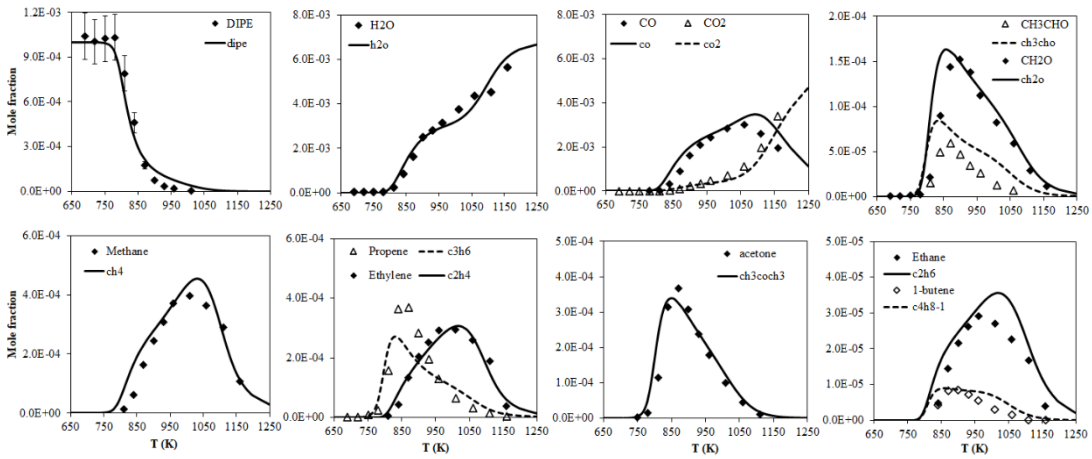

Figure 4. Mole fraction profiles for the φ = 1 mixture, P = 10 atm, $X_{0,fuel}$ = 0.1%, τ = 0.7 s (symbols: data, lines: simulations)

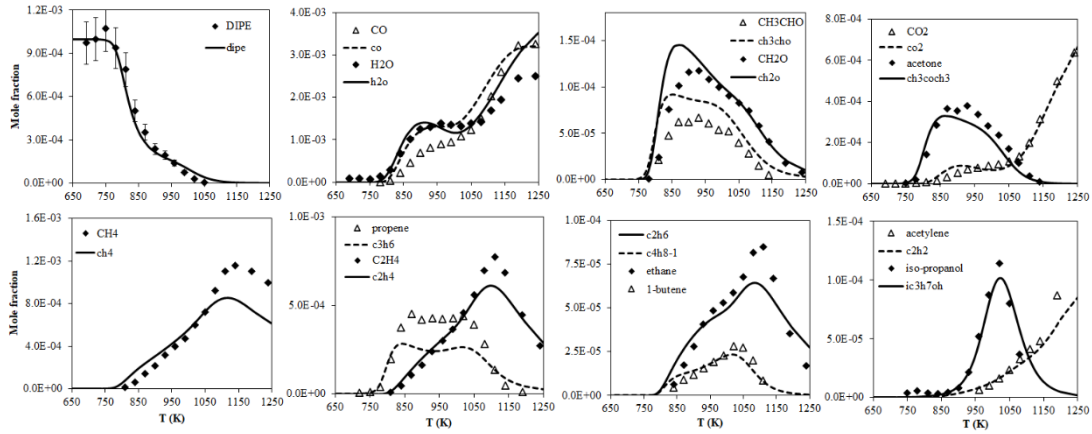

Figure 5. Mole fraction profiles for the φ = 2 mixture, P = 10 atm, $X_{0,fuel}$ = 0.1%, τ = 0.7 s (symbols: data, lines: simulations)

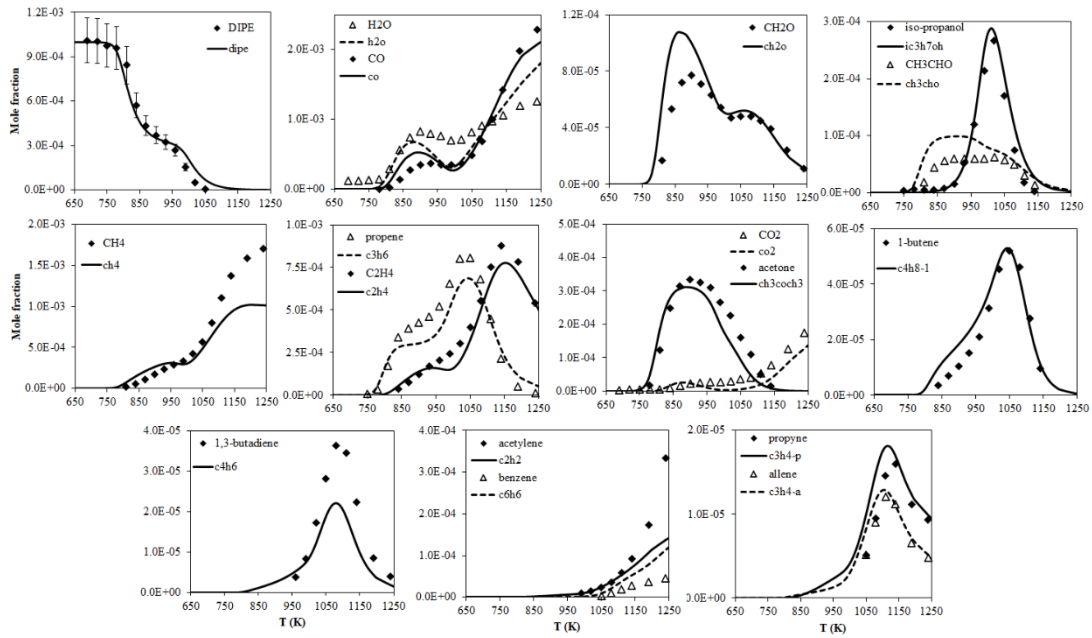

Figure 6. Mole fraction profiles for the φ = 4 mixture, P = 10 atm, $X_{0,fuel}$ = 0.1%, τ = 0.7 s (symbols: data, lines: simulations)

Experimental results (mole fraction profiles of reactant, intermediate and products) are presented in Figs 3–6. One can see from these figures that model–experiment comparison is generally quite good, often within 15–20%. Reactivity profiles and the intermediate distribution is substantially different between the lean (φ = 0.5) and the richest mixture (φ = 4). For example, no iso-propanol is observed at φ = 0.5 while iso-propanol formation with a peak of around 300 ppm can be seen at φ = 4 just below 1050 K. Meanwhile, an increased peak mole fraction of propene can also be observed at the same temperature. These intermediates are products of the molecular elimination reaction, which was the most important flux consuming the fuel under pyrolysis conditions [1]. In this sense, the richest mixture shows some similarity to pyrolysis. Note that while iso-propanol is exclusively produced via this pathway, propene is a common oxidation intermediate coming from other pathways as well. This is illustrated in Fig 7. Other production pathways for propene include the dehydration of iso-propanol and beta-scission of the (primary) fuel radical dipe2 ⇌ $iC_3H_7O + C_3H_6$.

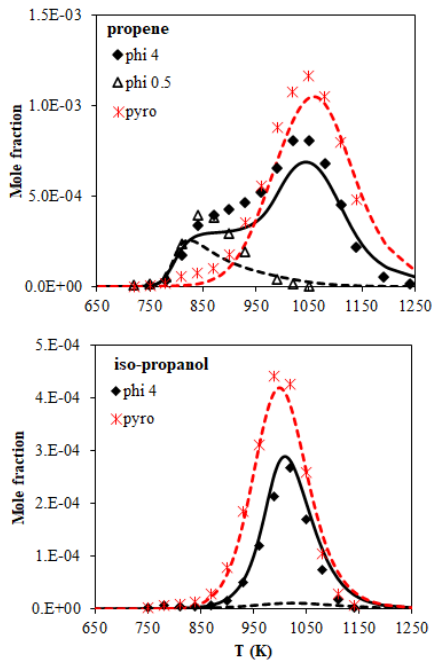

Figure 7. Comparison of propene and iso-propanol mole fraction profiles for the φ = 0.5 and 4 mixtures as well as the pyrolysis experiment [1]. P = 10 atm, τ = 0.7s.

3.2 Reaction path analysis

A reaction pathway analysis showing the initial decomposition pathways is given in Fig. 8.

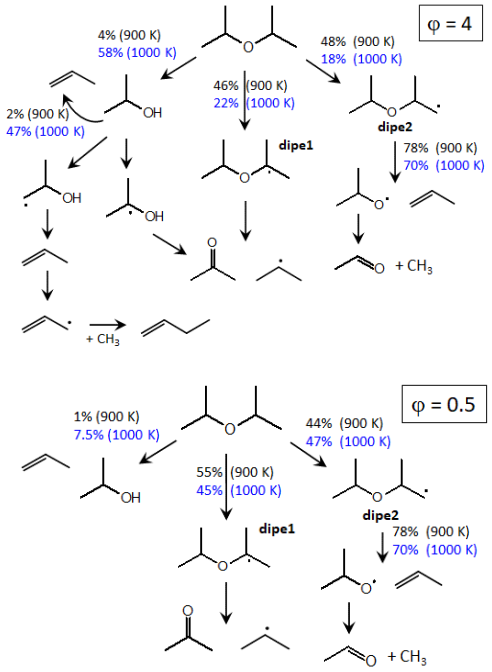

Figure 8. Reaction pathways for the φ = 0.5 and 4 mixtures at 900 K (black) and 1000 K (blue), P = 10 atm, τ = 0.7s.

For the φ = 4 mixture:

At 1000 K, the fuel mostly reacts via unimolecular decomposition while only 40% of the fuel consumption occurs through H-abstraction reactions producing dipe1 and dipe2. Among H-abstraction channels, abstraction by H atoms represent 20%, followed by CH_3 radicals, which represents 15% and that by OH radicals, representing a relatively small portion of 5-6%. Iso-propanol one of the products of the molecular reaction, which finally leads to the formation of allyl radicals. Recombination of allyl and methyl radicals yield 1-butene. This intermediate is observed with a peak around 55 ppm and owes its formation to this pathway. ~~Note that 1-butene is not observed at neither φ = 0.5 nor at φ = 1~~. Note that 1-butene is observed but in trace amounts (< 10 ppm) during the oxidation of lean and stoichiometric mixtures. This could be due to the combination of two phenomena linked to its formation and consumption. For example at 1000 K, allyl radicals combine with CH_3 radicals to a lesser extent when the mixture is lean (22%) than when it is rich (58%). Also, 1-butene consumption takes place via different pathways among which reactions with O atoms and OH radicals are the most important. At 1000 K and φ = 0.5, given the abundance of these radicals 1-butene is consumed at a more important rate than when φ = 4 (altogether accounting for 73% of its consumption at φ = 0.5, as opposed to a total of 32% at φ = 4). This may lead to the accumulation of 1-butene as the mixture gets richer.

On the other hand, at 900 K, temperature is not still high enough to overcome the barrier of the unimolecular reaction, representing only 4% of the reaction flux. The rest of the reaction flux corresponds to H-abstraction reactions: 33% by OH radicals, 38% by H atoms, 20% by CH_3 radicals and 5% by HO_2 radicals. The α–radical (dipe1) goes through β-scission to form acetone and the iso-propyl radical. At lower temperatures of interest (when T < 900 K) this is how acetone is formed. The β–radical (dipe2) mostly (78%) decomposes into the isopropoxy radical and propene, the remaining flux yields isopropyl vinyl ether and methyl radicals ($iC_3H_7OC_2H_3$ + CH_3). It is to be noted that neither $iC_3H_7OC_2H_3$ nor ~~a conjugated olefin of this ether~~ an unsaturated conjugate ether were observed experimentally under the present conditions.

For the φ = 0.5 mixture:

At any temperature, unimolecular decomposition is not significant. The fuel is consumed by hydrogen abstraction reactions. For this lean mixture, abstraction by OH radicals is more significant, representing a flux of 47% at 1000 K (as opposed to 5-6% for the φ = 4 mixture) followed by abstraction by H atoms representing 37% of the flux. At 900 K, hydrogen abstraction by OH radicals represents 63%,

while abstraction by H atoms represent about 25%. The fuel radicals undergo the same pathways with same branching ratios, as described under rich conditions.

A major part of acetaldehyde formation (60% under lean condition – 80% under fuel-rich condition) happens as a result of the β–scission of the dipe2 radical, which the model represents quite well at φ = 0.5 and 1 but over-predicts by a maximum of 50% when the mixture is fuel-rich. This may be due to the uncertainties in the estimated rate parameters for the H-abstraction reactions (especially by H-atoms that is important for the fuel-rich mixture) as well as the uncertainty related with the β-scission of the fuel radical, also estimated by analogy [20, 21]. A systematic theoretical study of the kinetics of these reactions would certainly be useful, not only for this fuel but also for the rest of the ether family as well as the alcohols.

3.3 Comparison with literature data

Figure 9 illustrates the JSR data at atmospheric pressure in [10], where reactants products and some important intermediates are represented. The pressure in that experiment was 1 atm, and the initial fuel mole fraction was 1%, only stoichiometric mixture was investigated by the authors. As can be seen in Fig 9, the present model can represent these data well. Note that authors' model showed similar discrepancies with their data as well. Iso-propanol is formed at T > 800 K, which the present model under-estimates while the authors' model represents it well. It is useful to note that given the differences in the operating conditions, no direct comparison can be made between the data in Fig 9 and the present work. The initial fuel mole fraction was 1% in their experiment (10 times higher than the present study) and the residence time was almost three times longer (2s vs 0.7s), which altogether enhance reactivity.

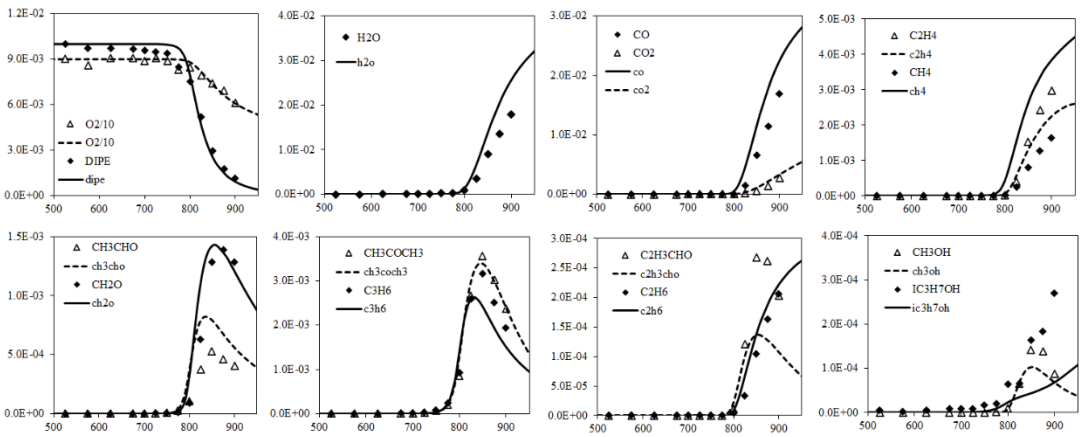

Figure 9. JSR data from literature [10] and comparison with the present model. Experimental conditions are: P = 1 atm, φ = 1, $X_{0,fuel}$ = 1%, τ = 2 s.

However, when the Fan et al. mechanism [10] is used to test our pyrolysis data where the unimolecular reaction dominates, iso-propanol is over-estimated and hence the overall reactivity. This can be observed in Fig 9. A more comprehensive comparison with our pyrolysis data and the literature model can be found in the supplementary material (Figures S1–S4).

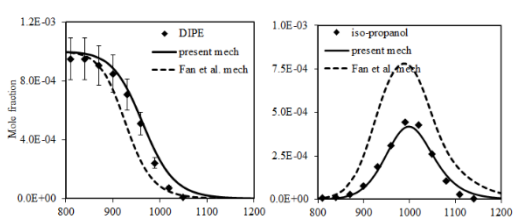

Fig. 10. Pyrolysis of DIPE [1], dashed lines represent the literature mechanism by Fan et al. [10]. Experimental conditions are: p = 10 atm, $X_{0,fuel}$ = 0.1%, τ = 0.7 s.

3.4 Comparison with other ethers

In our previous pyrolysis study [1], DIPE was found to be the most reactive among DEE, DPE and DBE, given its 12 primary C–H sites available for the molecular reaction whereas the other ethers have 4 available C–H sites. It was also expected that DIPE would be less reactive than DEE, DPE and DBE under oxidative conditions. Figure 11 illustrates the fuel conversion for diethyl (DEE), di-n-propyl (DPE), dibutyl (DBE) and di-iso-propyl ethers when φ = 2, at 10 atm and 0.7 s of residence time. At other equivalence ratios, the conclusion would be the same.

It is clear from this figure that among these ethers, the least reactive one is DIPE. The weakest C–H site in DIPE is the tertiary one with 2 equivalent bonds. The radical formed (dipe1) can add to molecular O_2 and undergo ROO• ⇌ •QOOH type of isomerization, as seen in the following scheme.

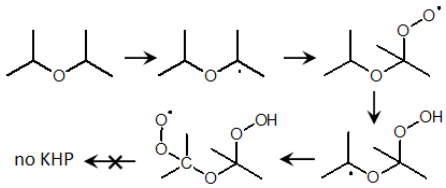

Second addition to O_2 forms the •OOQOOH radical, which cannot isomerize via a 6-membered transition state because of the quaternary C, and hence cannot form the corresponding ketohydroperoxides (KHP). Other possible internal H-transfers involve either 5- or 7-membered transition states, which are much less favorable. This in overall, reduces reactivity at low temperatures. At high temperatures, on the other hand, DIPE is less reactive than other ethers given that it has 12 equivalent, slightly enhanced (compared to n-alkanes) primary C–H bonds and only 2 weakened tertiary C–H sites. Its isomer, DPE, is much more reactive when T > 850 K, given its 4 equivalent weakened secondary C–H sites and only 6 primary C–H bonds, compared to DIPE.

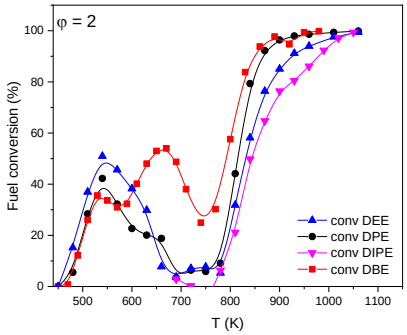

Figure 11. Comparison of fuel reactivity between DEE [5], DPE [3], DIPE (present study) and DBE [6] (lines are used to guide the eye).

4. Conclusions and perspective

In line with our previous studies, this work deals with the high-pressure oxidation of DIPE in a JSR, at 10 atm, with 0.1% initial fuel mole fraction, and at a constant residence time of 0.7 s. Four mixtures with equivalence ratios of 0.5–4 were investigated. Our results show that DIPE shows no reactivity at low temperatures and reactivity kicks off when the temperature is over 800 K. Therefore, no low temperature chemistry is included in the mechanism. While fuel decomposition is mainly due to hydrogen abstraction reactions (by H, OH and CH_3, and HO_2 (to a lesser extent), as the equivalence ratio increases the molecular reaction DIPE ⇌ iso-propanol + propene comes into picture. This can be seen with the φ = 4 mixture where a quasi-plateau is observed in the fuel profile between 850–950 K where we can also observe iso-propanol being produced and accumulated. This is also the case when φ = 2, but to a lesser extent.

As a perspective, and as the data on DIPE oxidation is quite scarce, data on global combustion properties such as ignition delay times can be envisaged, which would highlight a probably less significant pathway in this study. Also, a systematic theoretical study would be useful for metathesis reactions by H atoms and CH_3 radicals as well as fuel radical decompositions, which are often based on rough estimations.

Supplementary material

The kinetic mechanism and the experimental data are provided. A document with experiment/literature model comparison is also available.

References

[1] Z. Serinyel, G. Dayma, V. Glasziou, M. Lailliau, P. Dagaut, A pyrolysis study on C4–C8 symmetric ethers, Proc. Combust. Inst., 38 (2021) 329-336.

[2] N. Belhadj, R. Benoit, P. Dagaut, M. Lailliau, Z. Serinyel, G. Dayma, Oxidation of di-n-propyl ether: Characterization of low-temperature products, Proc. Combust. Inst., 38 (2021) 337-344.

[3] Z. Serinyel, M. Lailliau, G. Dayma, P. Dagaut, A high pressure oxidation study of di-n-propyl ether, Fuel, 263 (2020) 116554.

[4] N. Belhadj, R. Benoit, P. Dagaut, M. Lailliau, Z. Serinyel, G. Dayma, F. Khaled, B. Moreau, F. Foucher, Oxidation of di-n-butyl ether: Experimental characterization of low-temperature products in JSR and RCM, Combust. Flame, 222 (2020) 133-144.

[5] Z. Serinyel, M. Lailliau, S. Thion, G. Dayma, P. Dagaut, An experimental chemical kinetic study of the oxidation of diethyl ether in a jet-stirred reactor and comprehensive modeling, Combust. Flame, 193 (2018) 453-462.

[6] S. Thion, C. Togbé, Z. Serinyel, G. Dayma, P. Dagaut, A chemical kinetic study of the oxidation of dibutyl-ether in a jet-stirred reactor, Combust. Flame, 185 (2017) 4-15.

[7] M.D. Boot, M. Tian, E.J.M. Hensen, S. Mani Sarathy, Impact of fuel molecular structure on auto-ignition behavior – Design rules for future high performance gasolines, Prog. Energy Combust. Sci., 60 (2017) 1-25.

[8] A. Arteconi, A. Mazzarini, G. Di Nicola, Emissions from Ethers and Organic Carbonate Fuel Additives: A Review, Water, Air, & Soil Pollution, 221 (2011) 405.

[9] A. Goldaniga, T. Faravelli, E. Ranzi, P. Dagaut, M. Cathonnet, Oxidation of oxygenated octane improvers: MTBE, ETBE, DIPE, and TAME, Symp. (Int.) Combust., 27 (1998) 353-360.

[10] X. Fan, W. Sun, Z. Liu, Y. Gao, J. Yang, B. Yang, C.K. Law, Exploring the oxidation chemistry of diisopropyl ether: Jet-stirred reactor experiments and kinetic modeling, Proc. Combust. Inst., 38 (2021) 321-328.

[11] J. Hashimoto, J. Hosono, K. Shimizu, R. Urakawa, K. Tanoue, Extinction limits and flame structures of ETBE, DIPE and TAME non-premixed flames, Proc. Combust. Inst., 36 (2017) 1439-1446.

[12] A. Uyumaz, B. Aydoğan, A. Calam, F. Aksoy, E. Yılmaz, The effects of diisopropyl ether on combustion, performance, emissions and operating range in a HCCI engine, Fuel, 265 (2020) 116919.

[13] C.-W. Zhou, J.M. Simmie, H.J. Curran, An ab initio/Rice-Ramsperger-Kassel-Marcus study of the hydrogen-abstraction reactions of methyl ethers, H3COCH3-x(CH3)x, x = 0-2, by [radical dot]OH; mechanism and kinetics, PCCP, 12 (2010) 7221-7233.

[14] J. Zádor, J.A. Miller, in: 7th US National Techical Meeting, Combust. Inst., Combust. Inst., Atlanta, USA, 2011, pp. 483-488

[15] C.-W. Zhou, J.M. Simmie, H.J. Curran, Rate constants for hydrogen-abstraction by OH from n-butanol, Combust. Flame, 158 (2011) 726-731.

[16] P. Seal, E. Papajak, D.G. Truhlar, Kinetics of the Hydrogen Abstraction from Carbon-3 of 1-Butanol by Hydroperoxyl Radical: Multi-Structural Variational Transition-State Calculations of a Reaction with 262 Conformations of the Transition State, The Journal of Physical Chemistry Letters, 3 (2012) 264-271.

[17] A.T. Droege, F.P. Tully, Hydrogen atom abstraction from alkanes by hydroxyl. 5. n-Butane, The Journal of Physical Chemistry, 90 (1986) 5937-5941.

[18] J. Mendes, C.-W. Zhou, H.J. Curran, Rate Constant Calculations of H-Atom Abstraction Reactions from Ethers by HȮ2 Radicals, The Journal of Physical Chemistry A, 118 (2014) 1300-1308.

[19] P. Glarborg, R.J. Kee, J.F. Grcar, J.A. Miller, PSR: A Fortran Program for Modeling Well-Stirred Reactors, Report No. SAND86-8209, Sandia National Laboratories, Albequerque, NM, 1986.

[20] Y. Sakai, J. Herzler, M. Werler, C. Schulz, M. Fikri, A quantum chemical and kinetics modeling study on the autoignition mechanism of diethyl ether, Proc. Combust. Inst., 36 (2017) 195-202.

[21] H.J. Curran, Rate constant estimation for C1 to C4 alkyl and alkoxyl radical decomposition, Int. J. Chem. Kinet., 38 (2006) 250-275.